Crystal Structures and Photoelectron Spectra of Some Trimethanoanthracenes, Tetramethanonaphthacenes, and Pentamethanopentacenes. Experimental Evidence for Laticyclic Hyperconjugation

Michael N. Paddon-Row *
Department of Organic Chemistry, University of New South Wales, P.O. Box 1, Kensington, N.S.W. 2033, Australia
Lutz M. Englehardt, Brian W. Skelton, and Allan H. White
School of Chemistry, University of Western Australia, Nedlands, W.A. 6009, Australia
Flemming S. Jørgensen
Royal Danish School of Pharmacy, Department of Chemistry BC, 2, Universitetsparken, DK-2100, Copenhagen, Denmark
Harish K. Patney
Department of Chemistry, New South Wales Institute of Technology, P.O. Box 123, Broadway, N.S.W. 2007, Australia

Photoelectron (p.e.) spectra of the series of dienes (4), (10), (11a)—(13a), and crystal structures for the dodecachlorodienes(11b)—(13b) are reported. The spectra revealed large π-splitting energies of 0.32 and 0.52 eV for (4) and (11a) respectively. The value of (4) is attributed to the presence of orbital interactions through six σ bonds (OIT-6-B), and this, taken with the p.e. data for the dienes (1)—(3), provides convincing evidence for the long-range nature of OIT-n-B. The larger π-splitting energy of 0.52 eV observed for (11a), compared with (4), has been explained in terms of the presence of two reinforcing orbital interactions: OIT-6-B and a new variant of hyperconjugation, called laticyclic hyperconjugation, in which the π MOs of the double bonds mix with the $_w\pi$ MO of the central CH_2 bridge of (11a). The surprisingly large π-splitting energy of 0.29 eV observed for (12a) is also due largely to laticyclic hyperconjugation involving both pairs of symmetry adapted $_w\pi$ MOs of the CH_2 bridges. No π-splitting energy could be detected in the p.e. spectrum of (13a). From the crystal structures of (11b)—(13b), it was found that the distance between neighbouring CH_2 groups, and between a double bond and its closest CH_2 neighbour is about 3 Å in all three compounds. HF/STO-3G calculations on model ethene $\cdots$ $(CH_4)_n$ $\cdots$ ethene complexes suggest that laticyclic interactions, like OIT-n-B, are very long-range processes, the predicted π-splitting energies amounting to *ca.* 10^{-3} eV for two double bonds separated by *ca.* 33 Å. The relevance of these orbital interactions to biological electron-transfer processes is briefly discussed.

Recent photoelectron (p.e.) and electron transmission (e.t.) spectroscopic studies of the series of polymethano aromatic dienes (1)—(4),[1] and the corresponding dibenzo analogues,[1c] revealed the presence of large splitting energies between the π-type MOs. Such splitting energies were attributed to orbital interactions through bonds (OITB),[2–4] rather than to interactions of the through-space type (OITS),[2] on account of the long-range nature of the splitting energies. For example, the p.e. spectrum of (4) displayed two π ionization bands that were separated by 0.32 eV.[1d] This energy difference may be equated to the $\pi - \pi$ splitting energy, ΔE_π, assuming the validity of Koopmans' theorem.[5] Considering that the double bonds of (4) are separated by *ca.* 7.5 Å, such a large splitting energy could not be caused by OITS which are assumed to be negligible (*i.e.* $< 10^{-3}$ eV) for interorbital separations greater than 7 Å.

The dependence of the magnitude of OIT-n-B on the number, n, of relaying σ bonds for the series (1)—(4) was found approximately to follow the exponential form:[6]

$$\ln \Delta E_\pi = -0.46n + 1.56 \qquad (1)$$

from which it can be predicted that the splitting energy is attenuated only slowly with increasing values of n, being *ca.* 10^{-3} eV even for n as large as 18 or, equivalently, for an inter-π-orbital separation of 23 Å. This long-range nature of OIT-n-B may have important applications to electron-transfer processes, many of which are known to take place extremely rapidly, even for donor-acceptor distances as large as 13 Å.[7–9] It seems reasonable, therefore, that mutual coupling of the π MOs of the donor and acceptor moieties with the intervening σ framework, as in OITB, could facilitate long-range electron-transfer reactions. Indeed, the results of our recent kinetic studies of photo-induced electron-transfer in a series of rigid alicyclic compounds strongly support this conjecture.[8,9]


(1)

(2)

(3)

(4)

(5)

(6)

(7)
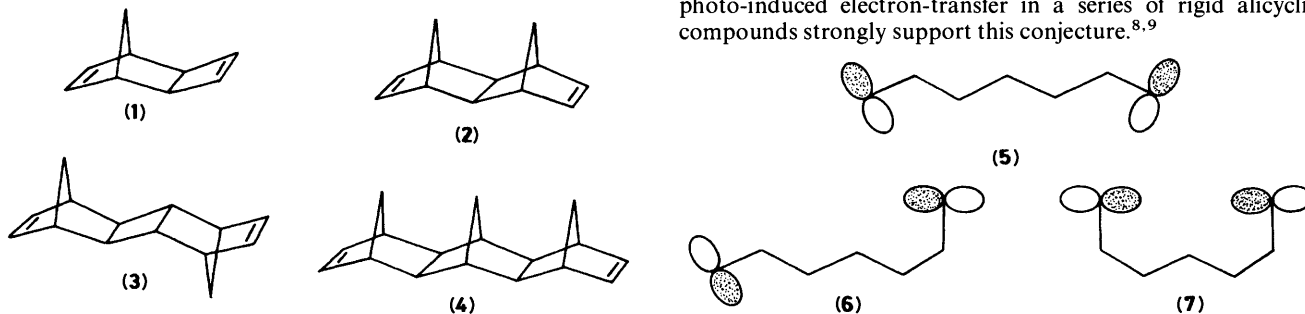
The pioneering (extended Huckel) calculations of Hoffmann, Imamura, and Hehre[10] predicted that the magnitude of through-bond interactions depends not only on the length of the σ framework but also on the conformation of that frame, being optimal for the all-*trans*, or antiperiplanar, conformation of the σ-bonds. Thus, coupling through six bonds is predicted to decrease along the series (5) > (6) > (7). Our experimental finding that ΔE_π is considerably greater for the all-*trans* diene (2) (0.87 eV[1b]) than for (8) (0.44 eV[11]), having a sickle arrangement of four σ bonds, supports the Hoffmann prediction, at least for the case of OIT-4-B. Of course, OIT-4-B in the U-shaped diene (9) are predicted to be even weaker than in (8). However, the measured value of ΔE_π for (9) was found to be 1.26 eV.[11] The unusually large value of ΔE_π in (9) was attributed to the presence of direct through-space interactions between the proximate double bonds which reinforce (and swamp) the weaker OIT-4-B.[11]

(8)   (9)

(10)
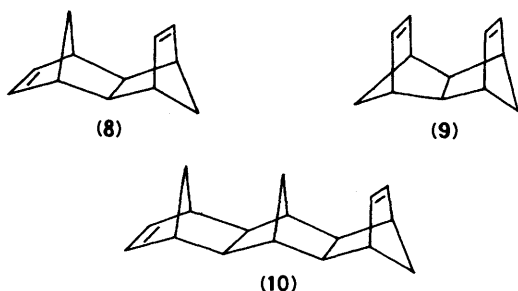
In order to explore further experimentally the Hoffmann 'all-*trans*' rule, it was decided to extend the investigations to include dienes (4), (10), and (11a), in which the double bonds are separated by six σ bonds. This series would provide a more stringent test of the all-*trans* rule on account of the fact that direct through-space interactions between the double bonds in the U-shaped diene (11a) should be negligible. This objective of the work was not achieved, however, because the experimental ΔE_π values for the dienes (10) and (11a) were found to be larger than that for (4).[1d] This unexpected result was attributed to the presence of a novel variant of through-bond interactions, called laticyclic hyperconjugation,[12,13] in which the π-systems of (11a) couple with the pseudo-π ($_\psi\pi$) MO of the bridging CH_2 group. Model *ab initio* MO calculations indicated that laticyclic hyperconjugation could extend over large distances, being transmitted through a series of CH_2 units as in (12a) and (13a).[13] An orbital representation of this interaction is shown by (17).

(11) a; X = H
b; X = Cl

(12) a; X = H
b; X = Cl

(13) a; X = H
b; X = Cl
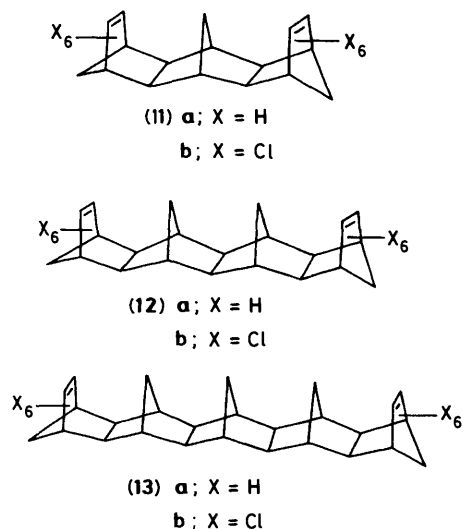
The predicted long-range nature of laticyclic hyperconjugation, and its obvious potential relevance to electron-transfer processes, makes it worthy of further experimental investigation. Some p.e. spectral data on dienes (4), (10), (11a), and (12a) have been reported in communication form.[1d,12] Herein, we report in more detail the results of those studies, together with p.e. data for (13a). We have also determined the crystal structures of the dodecachlorodienes (11b), (12b), and (13b), in order to gain more information about the geometrical relationships between the CH_2 groups and the double bonds in these molecules. Although it would have been better to have determined the crystal structures of the parent hydrocarbons, (11a), (12a), and (13a), we were unable to produce X-ray quality crystals, that were not twinned, from any of these these compounds. However, the overall geometries of these compounds, particularly with respect to the geometrical relationships between the CH_2 groups and the double bonds, should be practically identical to those of the corresponding chlorinated analogues (11b)—(13b).
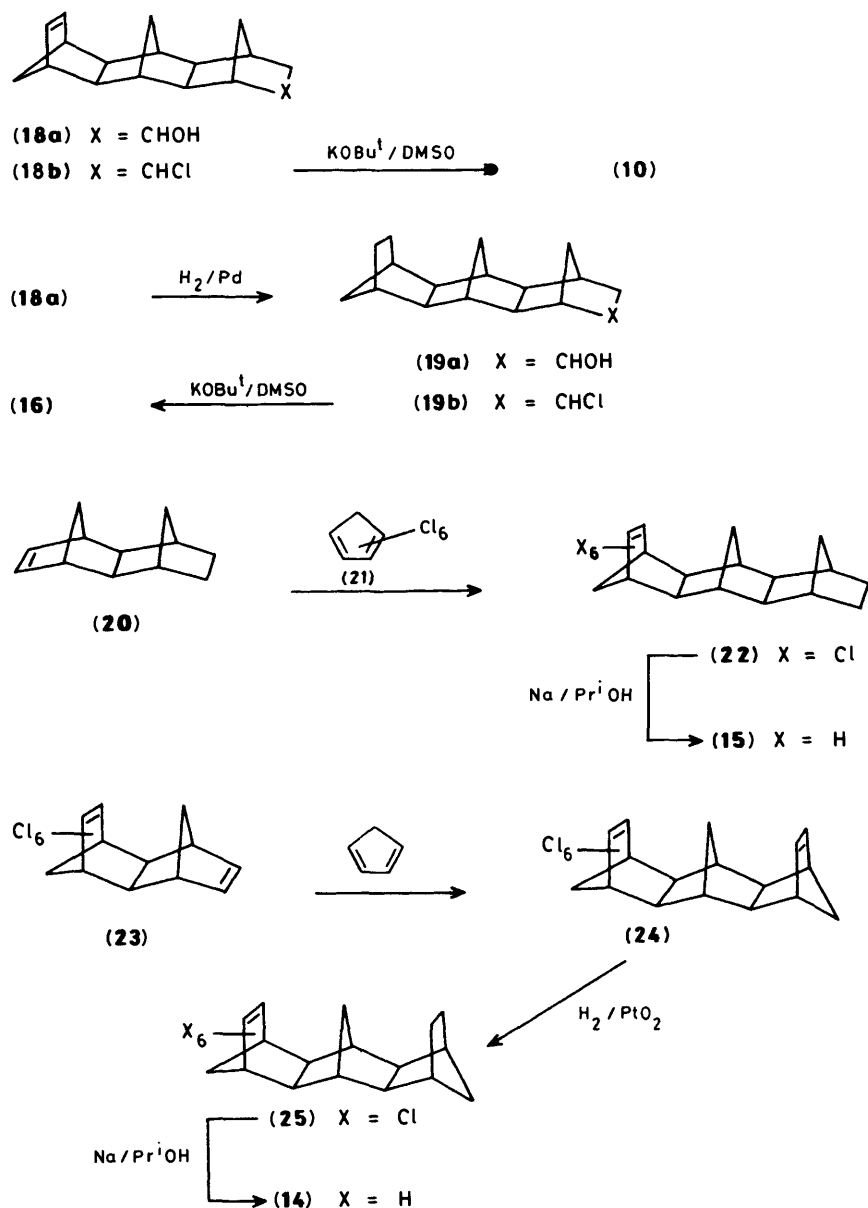

(14)   (15)

(16)

(17)
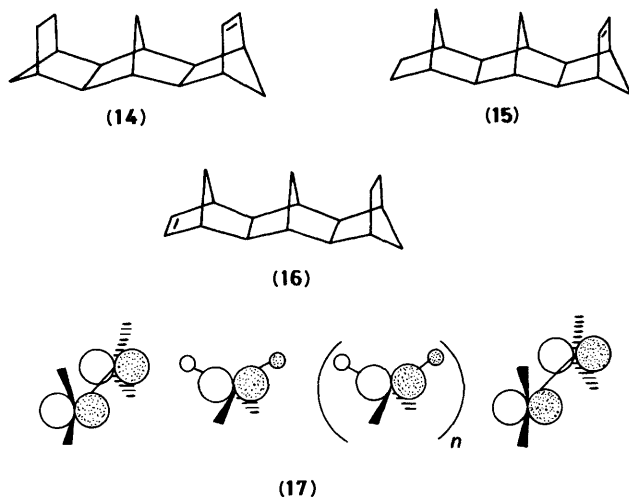
Experimental

Syntheses.—The syntheses of the dienes (4), (11)—(13) have been described elsewhere.[6] Synthetic routes to diene (10) and monoenes (14)—(16) are outlined in the Scheme.

(1α,4α,4aβ,5β,8β,8aβ,9α,9aβ,10α,10aβ)-1,4,4a,5,8,8a,9,9a,10,-10a-*Decahydro*-1,4:5,8:9,10-*trimethanoanthracene* (10).—A solution of the chloro compound (18b)[6] (531 mg, 2.0 mmol) in anhydrous dimethyl sulphoxide (DMSO) (10 ml) containing potassium t-butoxide (KOBu^t) (336 mg, 3.0 mmol) was stirred under N_2 at 25 °C for 18 h. The mixture was poured onto ice–water (*ca.* 30 g) and the resulting solution was extracted with ether (3 × 20 ml). The combined ether extracts were washed successively with ice-cold water (3 × 20 ml) and brine (20 ml). Evaporation of the ether gave a light brown oil. Chromatography of this oil (neutral alumina, hexane) gave a white solid, which was further purified by vacuum sublimation (120 °C/0.2 mmHg) to give (10) (137 mg, 61%), m.p. 137—139 °C (Found: C, 90.9; H, 9.1. $C_{17}H_{20}$ requires C, 91.0; H, 9.0%); δ (60 MHz; CDCl$_3$) 1.0 (d, *J* 10 Hz, 2 H), 1.25 (br s, 4 H), 1.48 (d, *J* 8 Hz, 2 H), 1.80—2.12 (m, 6 H), 2.65 (m, 2 H), 2.80 (m, 2 H), 5.93 (t, *J* 2 Hz, 2 H), and 6.15 (m, 2 H).

(1α,4α,4aα,5α,8α,8aα,9β,9aα,10β,10aα)-1,4,4a,5,6,7,8,8a,9,9a-10,10a-*Dodecahydro*-1,4:5,8:9,10-*trimethanoanthracene* (14).—A mixture of aldrin (23) (14.6 g, 40 mmol) and freshly cracked cyclopentadiene (10.6 g, 0.16 mol) was heated in a sealed tube

(18a) X = CHOH

(18b) X = CHCl

KOBu^t/DMSO $\longrightarrow$ **(10)**

(18a) $\xrightarrow{\text{H}_2/\text{Pd}}$

(19a) X = CHOH

(19b) X = CHCl

(16) $\xleftarrow{\text{KOBu}^t/\text{DMSO}}$

(20)

(21) $\longrightarrow$

(22) X = Cl

Na / Pr^{i}OH

(15) X = H

(23) $\longrightarrow$ **(24)**

H$_2$/PtO$_2$

(25) X = Cl

Na / Pr^{i}OH

(14) X = H

Scheme.

at 180—190 °C for 30 h. The cooled mixture was treated with chloroform and filtered, to remove insoluble polymeric material. The filtrate was evaporated to give an oil which, after chromatography (neutral alumina, hexane), yielded (**24**) (8.4 g, 48.7%) in a sufficiently pure form to be used for the next synthetic step; δ (60 MHz; CDCl₃) 1.27 (m, 2 H), 1.97 (m, 2 H), 2.37 (m, 4 H), 2.60 (m, 2 H), 2.97 (m, 2 H), and 6.03 (t, *J* 2 Hz, 2 H).

A solution of (**24**) (6.5 g, 15 mmol) in ethyl acetate (65 ml) containing PtO₂ (75 mg) was hydrogenated (25 °C, 1 atm) until the theoretical uptake of H₂ had occurred. The mixture was filtered and the filtrate evaporated to give (**25**) in nearly quantitative yield; δ (60 MHz; CDCl₃) 1.10—1.70 (br m, 10 H), 2.23 (m, 4 H), and 2.53 (s, 2 H). This compound was not purified further.

To a refluxing solution of (**25**) (4.33 g, 10 mmol) in THF (25 ml) and propan-2-ol (35 ml) under N₂ was slowly added small pieces of sodium metal (9.2 g, 0.4 mol). The refluxing mixture was stirred for a further 15 h. The cooled mixture was carefully treated with sufficient ethanol, to destroy any unchanged

sodium, and then diluted with ice-cold water (100 ml). Extraction of the resulting solution with ether (4 × 50 ml), and evaporation of the combined ether extracts (after washing with water and drying) gave crude (**14**). This material was sublimed (110 °C/2.0 mmHg) to give pure (**14**) (0.94 g, 41%), m.p. 146—148 °C (Found: C, 90.0; H, 9.9. C₁₇H₂₂ requires C, 90.2; H, 9.8%); δ (60 MHz; CDCl₃) 0.77—2.23 (br m, 18 H), 2.77 (m, 2 H), and 5.92 (t, *J* 2 Hz, 2 H).

(1α,4α,4aα,5β,8β,8aα,9β,9aα,10β,10aα)-1,4,4a,5,6,7,8,8a,9,9a,-10,10a-*Dodecahydro*-1,4:5,8:9,10-*trimethanoanthracene* (**15**).— A mixture of (**20**)¹⁴ (10.3 g, 64 mmol) and hexachlorocyclopentadiene (**21**) (27.3 g, 100 mmol) was heated in a sealed tube at 150 °C for 6 h. The resulting solid was recrystallized from acetone to give (**22**) (21.3 g, 76.4%); δ (60 MHz; CDCl₃) 0.73—2.03 (br m, 10 H), 2.10 (m, 2 H), 2.32 (m, 2 H), and 2.57 (s, 2 H).

Reductive dechlorination of (**22**) (8.67 g, 20 mmol) in boiling propan-2-ol (125 ml) with sodium (21.2 g, 0.92 mol) was carried out using identical conditions for the dechlorination of (**25**)

above. Recrystallization of the crude product, followed by sublimation (110 °C/2 mmHg) gave (15) (2.9 g, 64.2%), m.p. 138—140 °C (Found: C, 89.9; H, 9.9. $C_{17}H_{22}$ requires C, 90.2; H, 9.8%); δ (60 MHz; $CDCl_3$) 0.80 (d, J 10 Hz, 1 H), 0.97—2.27 (br m, 17 H), 2.72 (m, 2 H), and 5.85 (t, J 2 Hz, 2 H).

(1α,4α,4aβ,5β,8β,8aβ,9α,9aβ,10α,10aβ)-1,4,4a,5,6,7,8,8a,9,9a,-10,10a-*Dodecahydro*-1,4:5,8:9,10-*trimethanoanthracene* (16).—

A solution of (18a),[6] (1.5 g, 6.2 mmol) in ethyl acetate (40 ml) was hydrogenated using 10% Pd–C (70 mg) (25 °C, 1 atm). Filtration of the mixture, followed by evaporation of the filtrate, gave a quantitative yield of (19a) as a white solid which was not purified further. $\nu_{max.}(CCl_4)$ 3 635 (OH) cm⁻¹; δ (60 MHz; $CDCl_3$) 0.92 (d, J 11 Hz, 1 H), 0.93—2.27 (br m, 22 H inc. OH), and 4.07 (sym m, 1 H).

A solution of (19a) (1.20 g, 4.9 mmol) in freshly distilled hexamethylphosphoramide (HMPA) (8 ml) was cooled to 0 °C in a salt–ice bath. Freshly distilled thionyl chloride (0.82 g, 6.9 mmol) was added dropwise to this solution at such rate as to maintain the temperature between 0—10 °C. After the addition was completed, the solution was stirred for a further 6 h at room temperature, and then poured into ice–water (*ca.* 40 g). The solution was extracted with ether (4 × 40 ml) and the combined extracts were washed successively with ice–water (3 × 40 ml) and brine (40 ml). Evaporation of the dried ether solution gave a semi-solid product, presumably (19b), which was not purified further but subjected immediately to dehydrochlorination with potassium t-butoxide (1.1 g, 10 mmol) in anhydrous DMSO (25 ml) as described above for the preparation of (10) from (18b).

Table 1. Non-hydrogen atom co-ordinates of (11b)

Atom	x	y	z
C(1AB)	½	1	0.411(2)
C(1)	0.432 6(7)	1.067 4(7)	0.292(1)
C(2)	0.379 9(6)	0.973 3(7)	0.179 7(8)
C(3)	0.267 6(6)	0.905 2(7)	0.229 2(9)
Cl(3)	0.139 3(2)	0.975 9(2)	0.184 0(3)
C(3AB)	0.292 9(8)	0.792 9(8)	0.144(1)
Cl(3ABa)	0.184 4(2)	0.684 4(2)	0.180 8(4)
Cl(3ABb)	0.303 6(2)	0.803 6(2)	−0.064 2(3)
C(4)	0.282 7(7)	0.861 6(7)	0.394 3(8)
Cl(4)	0.213 3(2)	0.920 3(2)	0.554 8(3)

Table 2. Non-hydrogen atom co-ordinates of (12b)

Atom	Part A x	y	z	Part B x	y	z
C(1)	0.022 0(5)	−0.021 5(5)	0.203 8(3)			
C(2)	0.059 5(5)	0.093 8(5)	0.315 9(4)	0.059 4(5)	0.093 4(5)	0.183 9(4)
C(2AB)	0.012 3(4)	0.161 0(4)	0.249 3(6)			
C(3)	0.179 6(6)	0.091 0(5)	0.296 2(3)	0.179 7(5)	0.091 2(5)	0.203 9(3)
C(4)	0.255 5(6)	0.185 7(6)	0.315 2(4)	0.253 4(5)	0.188 3(6)	0.185 0(4)
Cl(4)	0.305 5(2)	0.185 1(2)	0.411 3(1)	0.302 1(2)	0.188 4(2)	0.088 4(1)
C(4AB)	0.339 7(4)	0.175 4(4)	0.249 8(5)			
Cl(4ABa)	0.437 5(1)	0.279 1(1)	0.249 2(1)			
Cl(4ABb)	0.410 2(1)	0.053 5(1)	0.249 8(2)			
C(5)	0.206 8(6)	0.290 5(7)	0.290 5(5)	0.205 0(6)	0.291 2(6)	0.213 2(5)
Cl(5)	0.149 8(2)	0.380 1(2)	0.351 6(2)	0.149 1(2)	0.383 3(2)	0.152 8(2)

Table 3. Non-hydrogen atom co-ordinates of (13b)

Atom	Part A x	y	z	Part B x	y	z
C(1AB)	0.476(2)	0.906(2)	0.572(2)			
C(1)	0.631(3)	1.036(2)	0.738(3)	0.557(2)	0.985(2)	0.594(2)
C(2)	0.747(2)	1.193(2)	0.854(2)	0.698(2)	1.161(2)	0.758(2)
C(3)	0.744(2)	1.254(2)	0.908(2)	0.679(2)	1.213(2)	0.774(2)
C(3AB)	0.612(2)	1.163(2)	0.773(2)			
C(4)	0.899(2)	1.426(2)	1.042(2)	0.847(2)	1.392(2)	0.942(2)
C(5)	0.959(2)	1.543(2)	1.147(2)	0.893(2)	1.502(2)	1.012(2)
Cl(5)	1.080 3(7)	1.651 4(6)	1.314 0(6)	0.902 0(6)	1.535 6(6)	0.966 9(7)
C(5AB)	1.040(2)	1.642(2)	1.183(2)			
Cl(5ABa)	1.129 9(6)	1.797 5(6)	1.306 7(6)			
Cl(5ABb)	1.200 9(6)	1.743 3(6)	1.286 8(6)			
C(6)	0.825(2)	1.466(2)	1.046(3)	0.786(2)	1.442(2)	0.966(2)
Cl(6)	0.736 4(6)	1.408 0(6)	1.031 0(6)	0.632 7(7)	1.341 9(7)	0.824 1(7)
C(2')	0.706(2)	1.050(2)	0.750(2)	0.651(2)	1.012(2)	0.646(2)
C(3')	0.630(3)	0.914(3)	0.657(4)	0.561(2)	0.869(3)	0.518(2)
C(3AB')	0.489(3)	0.782(3)	0.492(3)			
C(4')	0.757(2)	0.995(2)	0.722(2)	0.705(2)	0.960(2)	0.624(2)
C(5')	0.753(4)	0.919(4)	0.685(3)	0.675(3)	0.868(3)	0.541(3)
Cl(5')	0.860(1)	0.988(1)	0.823(1)	0.684(1)	0.873(1)	0.479(1)
C(5AB')	0.818(3)	0.966(3)	0.682(3)			
Cl(5ABa')	0.827 4(7)	0.897 4(7)	0.640 0(8)			
Cl(5ABb')	1.006 5(8)	1.170 9(8)	0.859 5(8)			
C(6')	0.583(4)	0.740(4)	0.508(5)	0.549(3)	0.721(3)	0.436(3)
Cl(6')	0.473(1)	0.609(1)	0.442(1)	0.364 9(8)	0.542 8(8)	0.233 4(8)

Figure 1. (a) Projection of the unit cell of (11b) down c. Thermal ellipsoids (20%) are shown for the non-hydrogen atoms in this, and subsequent structures, together with atom labelling. Hydrogen atoms, where shown, have arbitrary radii of 0.1 Å. (b) A single molecule of (11b)

Recrystallization of the crude product from acetone–ethanol, followed by sublimation (110 °C and 2 mmHg), gave (16) (0.35 g, 32%), m.p. 146—148 °C (Found: C, 89.9; H, 10.0. $C_{17}H_{22}$ requires C, 90.2; H, 9.8%); δ (60 MHz; $CDCl_3$) 0.87—2.30 (br m, 18 H), 2.63 (m, 2 H), and 6.07 (m, 2 H).

Structure Determinations.—Unique data were measured at *ca.* 295 K within $2\theta_{max}$. limits determined by the scope of the data using Syntex $P1$ and ENRAF-Nonius CAD4 four-circle diffractometers fitted with monochromatic Mo-K_α radiation sources ($\lambda = 0.71069$ Å) and operating in conventional $2\theta/\theta$ scan mode. N Independent reflections were measured, N_0 with $I > 3\sigma(I)$ being considered 'observed' and used in the least-squares refinement after solution of the structure by direct

methods. Anisotropic thermal parameters were refined for the non-hydrogen atoms; (x, y, z, $U_{iso})_H$ were constrained at estimated values. Residuals on $|F|$, R, and R' at convergence are given; statistical reflection weights were used with $\sigma^2(I) = \sigma^2(I)_{diff} + n_d \times 10^{-4}\sigma^4(I)_{diff}$. Neutral complex scattering factors were used.[15] Computation used the XTAL system of programs[16] implemented by S. R. Hall on a Perkin-Elmer 3240 computer. Skeletal atom numbering is shown in the Figures 1—3; atoms are numbered outwards from the centre of the skeleton with atoms A and B related by the (pseudo-)mirror plane along the length of the molecule and atoms AB in that plane. Where atoms related by the other (pseudo-)mirror plane are crystallographically independent they are denoted by primes.

Individual Data and Variations in Procedure.—(**11b**). C_{17}-H_8Cl_{12}, $M = 637.7$. Tetragonal, space group $P42_1m$ (D^3_{2d}, No. 113), $a = 11.582(9)$, $c = 8.458(5)$ Å; $U = 1\ 134(1)$ Å^3. $D_c = 1.87$ g cm^{-3}, $Z = 2$. $F(000) = 628$. $\mu_{Mo} = 13.6$ cm^{-1}; specimen: $0.14 \times 0.15 \times 0.25$ mm (no absorption correction). $2\theta_{max.} = 50°$. $N = 476$, $N_0 = 391$. $R = 0.036$, $R' = 0.038$ ($n_d = 3.5$) (both chiralities). Full matrix refinement.

(**12b**). $C_{22}H_{14}Cl_{12}$, $M = 703.9$. Tetragonal, space group $P4_12_12$ (D_4^4, No. 92), $a = 12.519(3)$, $c = 17.127(3)$ Å; $U = 2\ 684(1)$ Å^3. $D_c = 1.74$ g cm^{-3}, $Z = 4$. $F(000) = 1\ 400$. $\mu_{Mo} = 12.4$ cm^{-1}; specimen: $0.15 \times 0.15 \times 0.25$ mm. $2\theta_{max.} = 50°$. $N = 1\ 434$, $N_0 = 1\ 151$. $R = 0.036$, $R' = 0.041$ ($n_d = 4$) (both

chiralities). Full-matrix refinement; $(x, y, z)_H$ also refined. Additional pseudo-symmetry comprising a mirror plane within the molecule normal to c.

(**13b**). $C_{27}H_{20}Cl_{12}$, $M = 769.9$. Rhombohedral, space group $R3$ (C_{3i}^2, No. 148), $a = 25.322(5)$, $\alpha = 118.74(1)°$, $U = 4\ 702(2)$ Å^3. $D_c = 1.64$ g cm^{-3}, $Z = 6$. $F(000) = 2\ 340$. $\mu_{Mo} = 10.3$ cm^{-1}; specimen: hexagonal needle mounted up c, 0.06×0.5 mm (no absorption correction). $2\theta_{max.} = 40°$. $N = 2\ 914$, $N_0 = 1\ 544$. $R = 0.075$, $R' = 0.074$ ($n_d = 3.7$). 9×9 block diagonal refinement. High residuals and poor precision of the structure appear to be a consequence of limited crystal bulk and high thermal motion, with consequent limited accessible data.
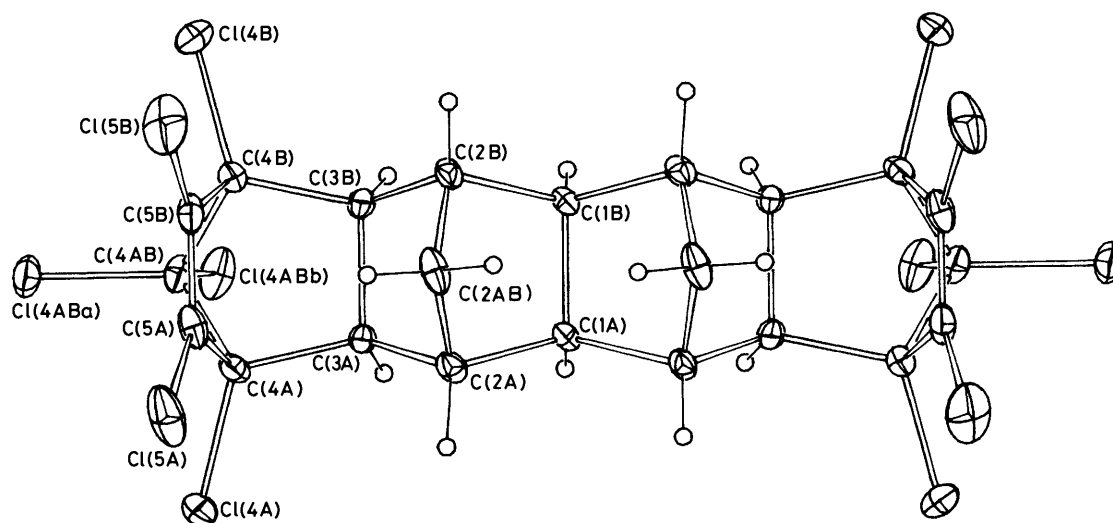

(a)
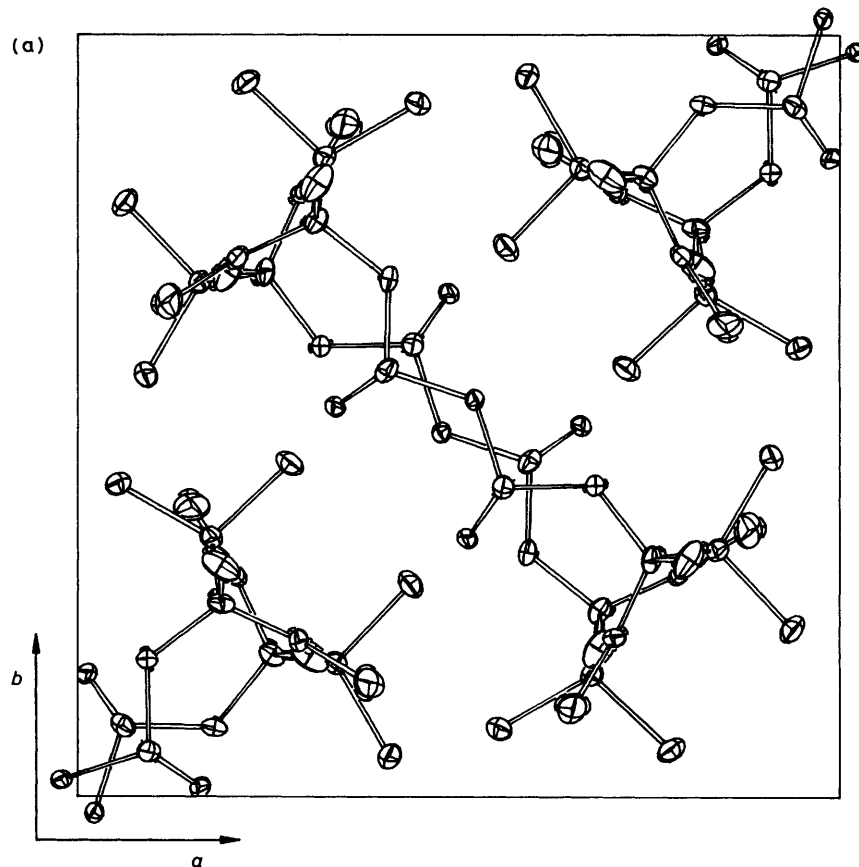
(b)
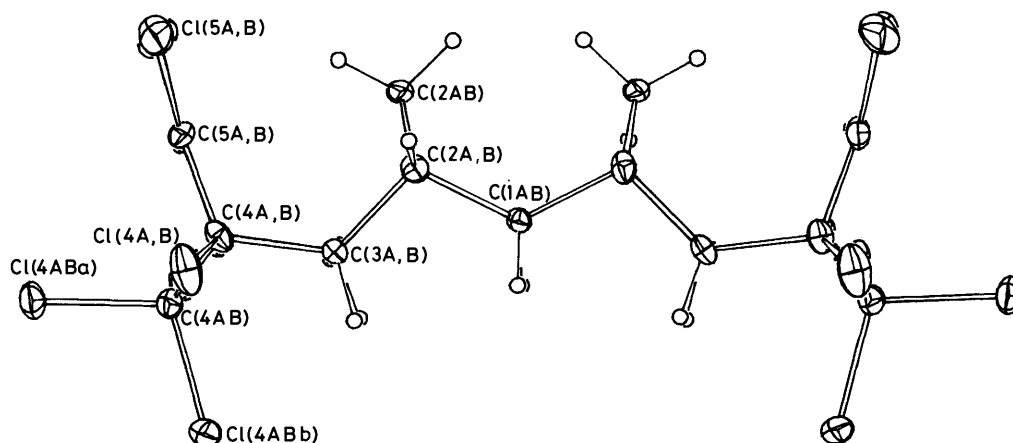
(c)

Figure 2. (a) Projection of the unit cell for (12b) down c. (b) and (c) A single molecule of (12b)

Thermal parameters, and hydrogen atom parameters for (11b)—(13b), have been deposited at the Cambridge Crystallographic Data Centre. Non-hydrogen interatomic distances and angles for (13b) are also contained in the deposted material.

Photoelectron Spectra.—The p.e. spectra were recorded on a Perkin-Elmer PS-18 spectrometer and calibrated with a mixture of argon and xenon gases. The recording temperatures for the compounds were: (4), 43—45 °C; (10), 43—44 °C; (11a), 47 °C; (12a), 106—107 °C; (13a), 135—136 °C; (14), 54 °C; (15), 55 °C; (16), 54 °C. The reported vertical ionization potentials are averages of four determinations, with the exception of that for (13a), which is the average of three determinations.

Results and Discussion

Structural Commentary.—Non-hydrogen atom co-ordinates for (11b), (12b), and (13b) are given in Tables 1—3 respectively. Non-hydrogen interatomic distances (Å) for (11b) and (12b) are listed in Tables 4 and 5 respectively, and the corresponding interatomic angles (Tables 6 and 7) and interplanar angles (Tables 8 and 9) are also listed. Non-hydrogen interatomic distances and interatomic angles for (13b) are not tabulated here owing to the poor precision of the structural data for this compound (*vide supra*), but they are included with the deposited material. The more reliable interplanar angles for (13b) are given in Table 10 ORTEP[17] drawings of (a) the unit cell, and (b) a single molecule for (11b)—(13b) are given in Figures 1—3 respectively.

The results of the three structure determinations are consistent with the expected stoicheiometries and connectivities. In all three cases the crystal symmetry is high, but the number of crystallographically imposed symmetry elements within the molecule diminishes in parallel with increase in molecular size. For the smallest compound (11b), the molecule lies disposed about the two-fold axis (1/2, 1, z) parallel to c at the intersection of the two associated mirror planes which contain it, with C(1AB) on that axis [Figures 1 (a and b)]. The molecule of (12b) [Figures 2 (a and b)] also lies disposed about a crystallographic

two-fold axis, but now this is the only crystallographically imposed symmetry element; in space group $P4_12_12$ this lies normal to the tetragonal four-fold axis (rather than parallel to it as was the case for (11b), along the *ab* face diagonal. Pseudo-symmetry, however, is strongly apparent in this molecule as the pseudo-mirror plane along the long axis of the molecule coincides almost exactly with the plane $z = 1/4$. Compound (13b) conforms to a trigonal rather than to a tetragonal crystal system. The molecule is devoid of any crystallographically imposed symmetry with thermal librational amplitudes very pronounced at one end; this, coupled with the imprecision of the determination, demands caution in consideration of features of molecular geometry.

Although basic geometrical parameters of bond lengths and angles are generally as expected, some features of interest may be noted for the two more precisely determined structures (11b) and (12b). In the skeleton of (11b) the C(1,2,3) string exhibits bond lengths that are greater than those expected for the tetrahedral norm. Similar, but rather less pronounced, distortions are evident in the analogous C(2,3,4) strings of (12b). The most significant variations in bond length, however, are those found in the carbon–chlorine distances, which have a spread of *ca.* 0.1 Å, the vinylic C–Cl lengths lying at about 1.7 Å, while the saturated C–Cl lengths are close to 1.8 Å. In the *gem*-dichloro pair at the ends of each molecule, the 'equatorial' C–Cl bond is consistently slightly longer than the corresponding 'axial' C–Cl bond. The difference is small, however, and of dubious significance, particularly in the absence of a correction for libration. The angle between these two chlorine atoms is less than the tetrahedral norm, a somewhat surprising result in view of the constraint of the bridgehead angle, which is diminished to less than 100° in each case: C(3A)–C(3AB)–C(3B) = 96° for (11b) and C(4A)–C(4AB)–C(4B) = 92° for (12b). The magnitude of the difference between the bridgehead angles in (11b) and (12b) is also notable, since the two halves of (12b) are identical with the two ends of (11b), and their geometries are generally similar in other respects.

Evident in all three molecules is a tendency toward curvature in the molecular frame which can be seen in the 'side-on' projections. This is a consequence of the difference in the

(a)

(b)

(c)
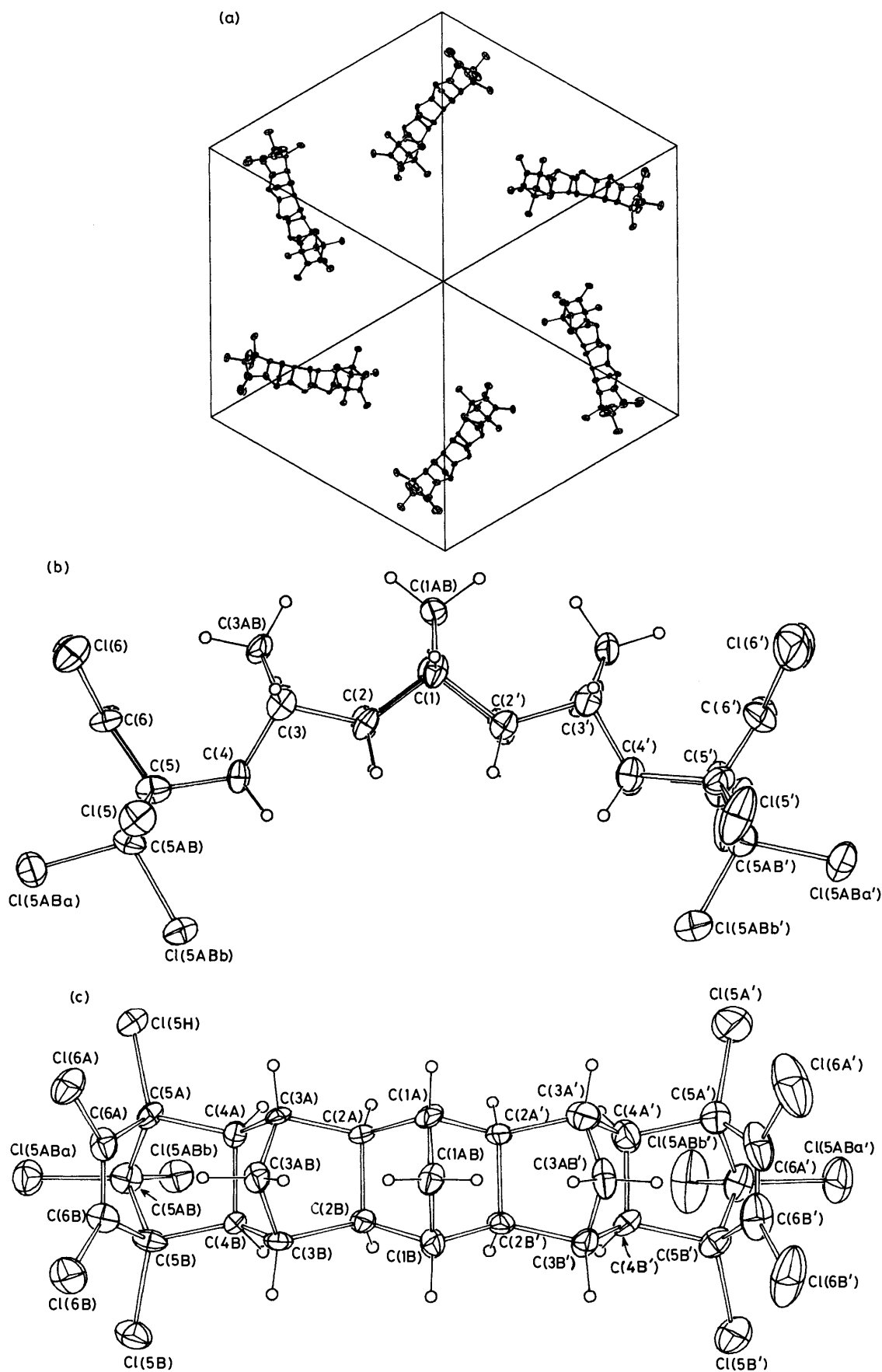
Figure 3. (a) Unit-cell contents of (13b) down hexagonal c. (b) and (c) A single molecule of (13b). Atoms A lie away from the reader, with the primed section of the molecule to the right

Table 4. Non-hydrogen interatomic distances (Å) of (11b)*

Atoms	Distance
C(1)–C(1AB)	1.49(1)
C(1)–C(2)	1.57(1)
C(2)–C(2)	1.53(1)
C(2)–C(3)	1.58(1)
C(3)–Cl(3)	1.739(8)
C(3)–C(3AB)	1.52(1)
C(3AB)–Cl(3ABa)	1.81(1)
C(3AB)–Cl(3ABb)	1.77(1)
C(3)–C(4)	1.50(1)
C(4)–C(4)	1.29(1)
C(4)–Cl(4)	1.718(7)

* Italicized atoms are symmetry related.

Table 5. Non-hydrogen interatomic distances (Å) of (12b). The two values in each entry are for parts A, B

Atoms	Distance
C(1A)–C(1B)	1.582(6)
C(1)–C(2)	1.563(9), 1.550(9)
C(2AB)–C(2)	1.54(1), 1.52(1)
C(2)–C(3)	1.541(10), 1.545(9)
C(3A)–C(3B)	1.581(8)
C(3)–C(4)	1.56(1), 1.561(10)
C(4)–Cl(4)	1.760(8), 1.763(7)
C(4)–C(4AB)	1.54(1), 1.56(1)
C(4AB)–Cl(4ABa,b)	1.786(5), 1.762(6)
C(4)–C(5)	1.50(1), 1.51(1)
C(5A)–C(5B)	1.32(1)
C(5)–Cl(5)	1.692(9), 1.700(9)

**Table 6.** Non-hydrogen interatomic angles (°) of (11b)*

Atoms	Angle
C(1)–C(1AB)–C(1)	95.4(10)
C(1AB)–C(1)–C(2)	104.3(6)
C(2)–C(1)–C(2)	100.1(7)
C(1)–C(2)–C(2)	102.5(6)
C(1)–C(2)–C(3)	120.5(6)
C(3)–C(2)–C(2)	103.2(6)
C(2)–C(3)–Cl(3)	114.2(5)
C(2)–C(3)–C(4)	108.7(6)
C(2)–C(3)–C(3AB)	98.2(6)
Cl(3)–C(3)–C(4)	117.7(6)
Cl(3)–C(3)–C(3AB)	117.6(6)
C(4)–C(3)–C(3AB)	97.7(6)
C(3)–C(3AB)–Cl(3ABa)	112.3(6)
C(3)–C(3AB)–Cl(3ABb)	115.4(6)
Cl(3ABa)–C(3AB)–Cl(3ABb)	105.7(5)
C(3A)–C(3AB)–C(3B)	95.9(7)
C(3)–C(4)–C(4)	108.8(6)
C(3)–C(4)–Cl(4)	123.3(6)
C(4)–C(4)–Cl(4)	127.7(6)

* Italicized atoms are symmetry related.

Table 7. Non-hydrogen interatomic angles (°) of (12b). The two values in each entry are for parts A, B

Atoms	Angle
C(1)–C(1)–C(2)	102.2(5), 103.0(5)
C(2)–C(1)–C(2)	121.0(5)
C(1)–C(2)–C(2AB)	103.3(5), 103.7(5)
C(1)–C(2)–C(3)	103.2(5), 103.3(5)
C(2AB)–C(2)–C(3)	103.0(5), 102.9(5)
C(2A)–C(2AB)–C(2B)	95.3(5)
C(2)–C(3)–C(3)	102.7(5), 102.7(5)
C(2)–C(3)–C(4)	122.2(5), 121.1(5)
C(3)–C(3)–C(4)	102.0(5), 102.1(5)
C(3)–C(4)–Cl(4)	114.2(5), 113.5(5)
C(3)–C(4)–C(4AB)	101.6(5), 100.4(5)
Cl(4)–C(4)–C(4AB)	115.8(5), 115.4(5)
C(3)–C(4)–C(5)	111.0(6), 111.3(6)
C(5)–C(4)–Cl(4)	114.2(5), 116.1(6)
C(5)–C(4)–C(4AB)	98.4(6), 98.0(6)
C(4A)–C(4AB)–C(4B)	92.0(5)
C(4)–C(4AB)–Cl(4ABa)	114.3(5), 113.3(5)
C(4)–C(4AB)–Cl(4ABb)	114.5(5), 115.9(5)
Cl(4ABa)–C(4AB)–Cl(4ABb)	106.6(3)
C(4)–C(5)–C(5)	107.1(7), 108.0(7)
C(4)–C(5)–Cl(5)	125.0(6), 123.5(6)
C(5)–C(5)–Cl(5)	127.3(7), 128.4(7)

Table 8. Interplanar angles (°) of (11b)*†
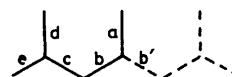
	b	c	d	e
a	128.2	74.2	9.5	135.5
b		125.9	61.2	7.2
c			115.3	118.7
d				126.0

* Defining atoms: a, C(1AB, 1, *1*); b, C(1, *1*, 2, *2*); c, C(2, *2*, 3, *3*); d, C(3, *3*, 4, *4*); e, C(3, *3*, 3AB). Italicized atoms are related by the mirror plane in the page. The b/b′ dihedral angle is 103.5°. † Typical e.s.d.s in this, and subsequent Tables, are of the order of 0.5°.

Table 9. Interplanar angles (°) of (12b)

	b	c	d	e	f
a	126.9	106.9	19.8	136.8	100.3
b		126.2	72.9	9.9	132.8
c			126.7	63.7	6.7
d				117.0	120.1
e					122.9

Defining atoms: a, 1A, 1B, 2A, 2B; b, 2A, 2B, 2AB; c, 2A, 2B, 3A, 3B; d, 3A, 3B, 4A, 4B; e, 4A, 4B, 5A, 5B; f, 4A, 4B, 4AB. The a/a dihedral angle is 126.3°.

magnitude between two different kinds of interplanar angles (see Tables 8—10). Thus, the angle between the two planes each containing four carbon atoms *within* the same methano aromatic unit (*i.e.* planes b and b′ of Table 8) is only *ca.* 106°, whereas that between corresponding planes on adjacent units (*i.e.* planes b and c of Table 8) is *ca.* 20° larger. This effect appears typical of polymethano aromatic systems, and is also evident in the crystal structures of aldrin[18] and dibenzo analogues of (11b).[19]
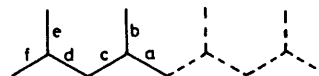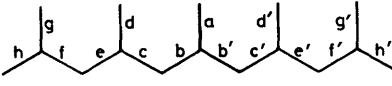
Inspection of the 'side-on' projections of (11b)—(13b) (Figures 1—3) also reveals a distinct tendency towards pyramidalization of the carbon–carbon double bonds in each molecule. The direction of pyramidalization is *endo*, relative to the norbornyl unit containing the double bond. The degree of pyramidalization, as measured by the angle between the planes

Table 10. Interplanar angles (°) of (13b). The two values in each entry are for unprimed and primed halves of the molecule respectively

	b	c	d	e	f	g	h
a	127.6, 128.2	76.6, 72.5	22.3, 21.4	149.6, 150.5	97.6, 94.6	34.9, 32.3	156.6, 157.5
b		129.0, 124.3	74.6, 73.1	22.1, 22.4	150.0, 146.4	92.8, 96.0	29.1, 29.4
c			125.6, 128.8	106.9, 102.0	21.0, 22.1	138.2, 139.7	99.9, 95.0
d				127.5, 129.2	75.4, 73.3	12.6, 11.0	134.5, 136.2
e					127.9, 124.0	65.1, 61.7	7.0, 7.0
f						117.2, 117.6	120.9, 117.0
							121.9, 125.3
g	The b/b' angle is 104.2°						

Defining atoms: a, C(1AB), C(1A,B); b, C(1A,B), C(2A,B); c, C(2A,B), C(3A,B); d, C(3A,B), C(3AB); e, C(3A,B), C(4A,B); f, C(4A,B), C(5A,B); g, C(5A,B), C(6A,B); h, C(5A,B), C(5AB).

containing the Cl–C=C–Cl and C–C=C–C atoms, is *ca.* 6° for **(11b)** and 7° for both **(12b)** and **(13b)**. *endo* Pyramidalization of double bonds in the norbornenyl system has been recently predicted,[20,21] and subsequently verified experimentally in several compounds.[19,22,23] The results reported herein provide further convincing testimony to the widespread occurrence of *endo* pyramidalization in polymethano aromatic compounds.

In consideration of non-bonded effects within **(12b)**, it is of interest to note that the right-hand hydrogen atom on C(2AB) [see Figure 2(b)] is only 1.70(7) Å from its symmetry-related neighbour. In this determination, the hydrogen atoms were refined, and in Figure 2(c) there is some suggestion of a consequent twist in the hydrogen atom disposition, thereby reducing the acute steric congestion which must result from the proximity of the two bridgehead CH_2 groups. This suggestion receives more substantial support from consideration of the orientation of the C(2AB) thermal tensor, which reflects the possible hydrogen atom twist.

The extremely short C–H ••• H–C non-bonded contact distance observed for the CH_2 groups in **(12b)** is comparable to that found (*ca.* 1.68 Å) between the indicated H atoms in **(26)**, also by X-ray crystallography.[24] A more accurate determination of this H ••• H distance in **(26)** by neutron diffraction revealed it to be 1.713(3) Å,[25] about 0.03 Å longer than the X-ray value. The corresponding H ••• H distance in **(12b)** is therefore more likely to be about 1.74 Å, which is still exceptionally short.[25]

(26)

(27)

(28)
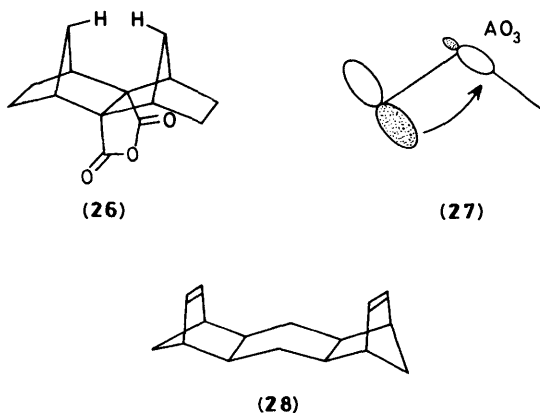
The distance of a bridgehead CH_2 group from the centre of the nearest double bond is about 2.95 Å in all three compounds. The distance between two adjacent bridgehead CH_2 groups in **(12b)** and **(13b)** is 3.06 and *ca.* 3.1 Å respectively. Thus, for the
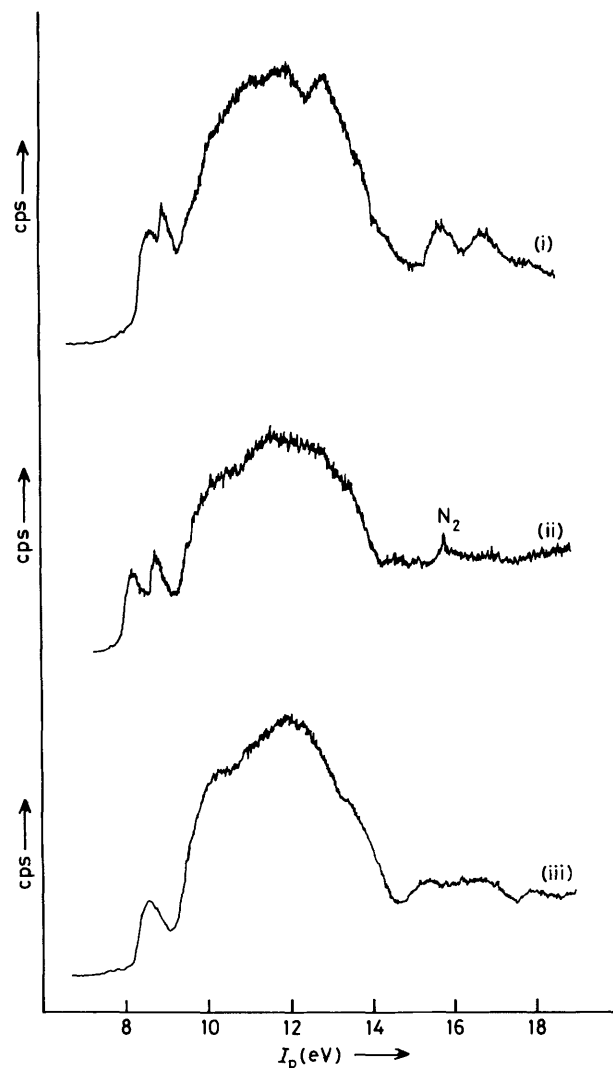
Figure 4. He[I] photoelectron spectra of (i) **(4)**, (ii) **(11a)**, and (iii) **(14)**

array of double bonds and bridgehead CH_2 groups in **(11b)**— **(13b)**, adjacent members of that array are separated by the same distance of *ca.* 3 Å. This separation is well within the sum of the van der Waals radii of 3.4 Å for two carbon atoms.[26]
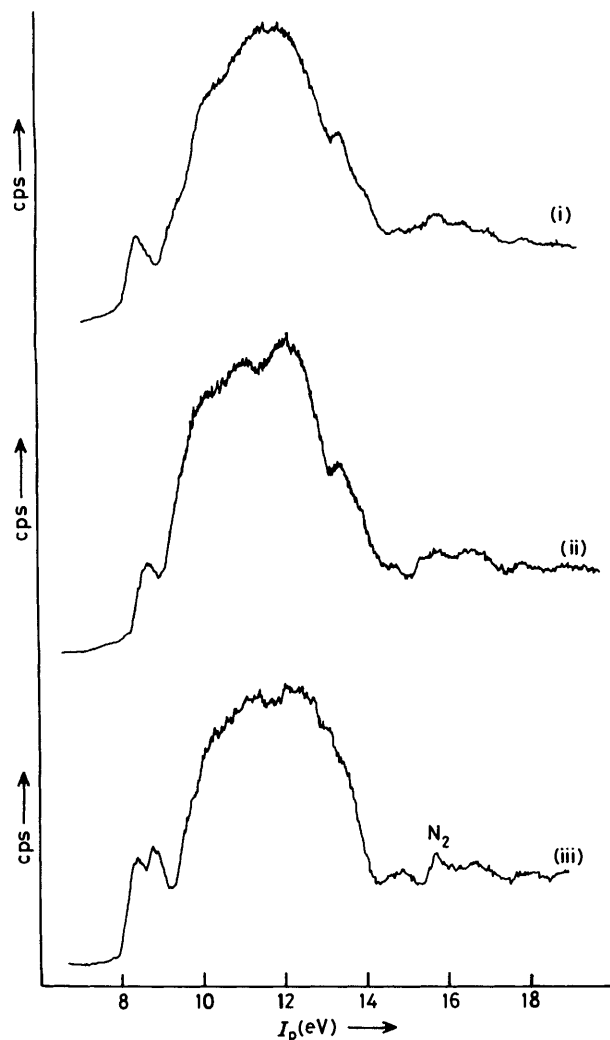
Figure 5. He[1] photoelectron spectra of (i) (15), (ii) (16), and (iii) (10)
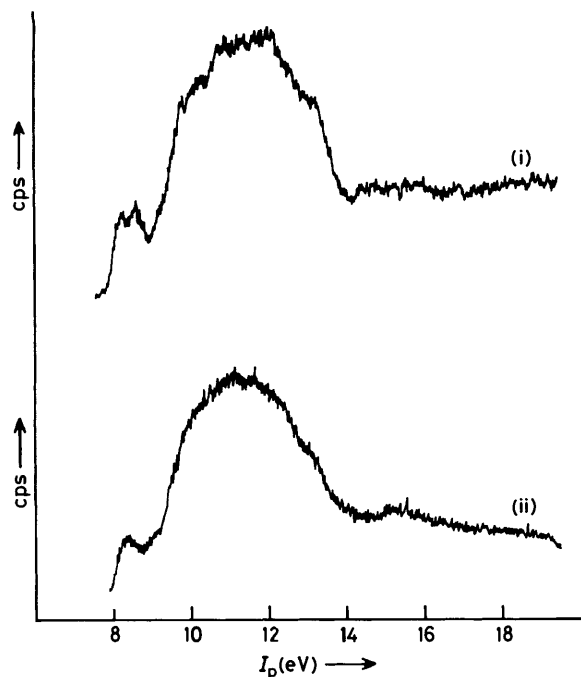
Figure 6. He[1] photoelectron spectra of (i) (12a) and (ii) (13a)

Table 11. Vertical π-ionization potentials, πI_p (eV), assignments,[a] and HF/STO-3G and PRDDO π-splitting energies, ΔE_π (eV)

Compd.	πI_p	Assignment	$\pi \Delta I_p$	ΔE_π STO-3G	ΔE_π PRDDO
(1)	8.65[b]	$\pi + \pi$[b]	1.15	1.36	
	9.80[b]	$\pi - \pi$[b]			
(2)	8.48[c]	$\pi - \pi$	0.87	0.89	0.75
	9.35[c]	$\pi + \pi$			
(3)	8.60[d]	$\pi + \pi$[d]	0.43	0.28	
	9.03[d]	$\pi - \pi$[d]			
(4)	8.58	$\pi - \pi$	0.32	0.31	0.17
	8.90	$\pi + \pi$			
(8)	8.46[e]	$\pi - \pi$	0.44	0.52	
	8.90[e]	$\pi + \pi$			
(10)	8.36	$\pi - \pi$	0.39		0.23
	8.74	$\pi + \pi$			
(11a)	8.24	$\pi - \pi$	0.52	0.51	0.49
	8.76	$\pi + \pi$			
(12a)	8.31	$\pi - \pi$	0.29		0.49
	8.60	$\pi + \pi$			
(13a)	8.41	$\pi + \pi; \pi - \pi$	$ca.$ 0		0.15
(14)	8.51				
(15)	8.47				
(16)	8.68				
(28)	8.63[f]	$\pi - \pi$	0.17	0.18	
	8.80[f]	$\pi + \pi$			

[a] Deduced from STO-3G and PRDDO MO calculations. [b] Ref. 1a. [c] Ref. 1b. [d] Ref. 1c. [e] Ref. 11. [f] G. D. Willett, personal communication to M. N. P.-R.

Photoelectron Spectra.—The photoelectron spectra of (4), (11a), and (14) are shown in Figure 4, those of (10), (15), and (16) in Figure 5, and those of (12a) and (13a) in Figure 6. Vertical π-ionization potentials (πI_p) are presented in Table 11. Although two distinct π-ionization bands could be seen in the p.e. spectra of (4), (11a), (12a), and (10), from which the πI_p-splitting energies $\pi \Delta I_p$, were obtained, only a single broad hump, corresponding to π ionization, was observed in the p.e. spectrum of (13a). It appears that the FWHM (full width at half-maximum height) of each of the two πI_p bands of (11a) and (12a) are nearly identical to the FWHM of the 8.41 eV band of (13a). The two π levels of (13a) are therefore nearly degenerate. We hesitate to give an upper limit to the magnitude of any splitting of the π levels that could be present in the p.e. spectrum of this compound because the shape of the πI_p band is heavily distorted by the large σ-envelope.

Assignments of the π ionization bands are given in Table 11. These were made on the basis of Hartee–Fock STO-3G (HF/STO-3G) and partial retention of diatomic differential overlap (PRDDO)[27] MO calculations, which were carried out on molecular geometries optimized by Allinger's MM2 molecular mechanics program.[28]

The interpretation of the p.e. data will be made within the context of Koopmans' theorem.[5] This is reasonable because we are interested mainly in *differences* between energy levels and not in their absolute values. Consequently, agreement between experimental $\pi \Delta I_p$ and computed ΔE_π values should be good, since electronic relaxation and correlation effects are expected largely to cancel out in ΔE_π. Indeed, this appears to be the case for the HF/STO-3G calculations. With the exception of (3), the agreement between ΔE_π and $\pi \Delta I_p$ is very good (Table 11). The PRDDO results, however, are generally in much worse agreement with the experimental data.

Through-bond Interactions in (1)—(4).—The πI_p correlation diagram for these compounds, in which the double bonds are
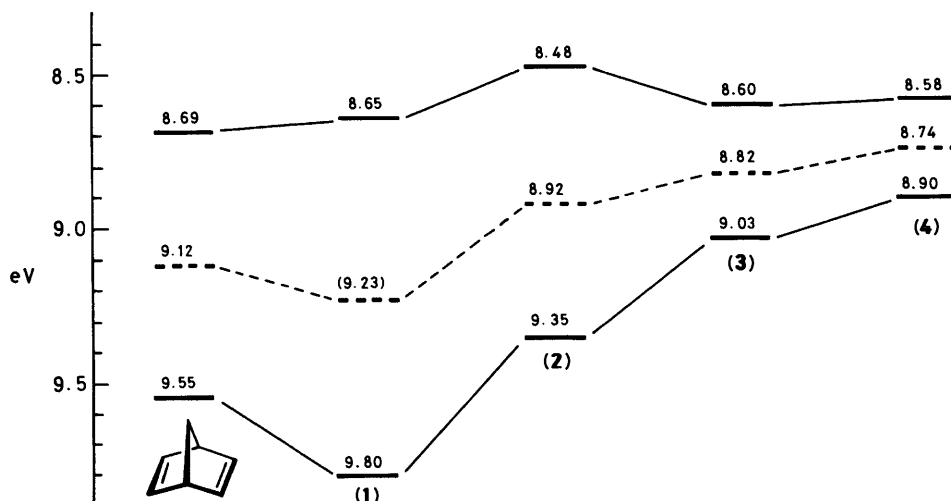
Figure 7. πI_p Correlation diagram for 8,9,10-trinorbornadiene, (1), (2), (3), and (4). The dashed line connects the means of the πI_p values

connected by an all-*trans* alignment of σ bonds, is shown in Figure 7. From the crystal structures for (12b) and (13b) the distance between the double bonds in (2) and (4) can be estimated to be 4.8 and 6.9 Å respectively. Clearly, through-space interactions in (2)—(4) are negligible. The very large $\pi\Delta I_p$ values observed for these compounds must therefore be attributed to through-bond interactions. The π-splitting energy of 0.32 eV, measured for (4), is the largest ever recorded for OIT-6-B. The decay of the π-splitting energy with increasing number, n, of relaying σ bonds is quite mild, a rough quantitative description of which is provided by equation (1) ($\pi\Delta I_p = |\Delta E_\pi|$ by Koopmans' theorem). The predicted π-splitting energy for the as yet unsynthesized eight-bond diene homologue of (4) is *ca.* 0.12 eV, which is probably too small to be measured accurately by p.e. spectroscopy, but which, nevertheless, is impressively large considering the length of the σ bond relays.

Interestingly, the decay of $\pi\Delta I_p$ along the series of dienes (1)—(4) is due largely to changes in the energy of the higher-energy I_p band, the energy of the lower-energy band remaining roughly constant (see Figure 7). This is also reflected in the HF/STO-3G calculations which reveal a marked increase in the energy of the lower π level, but a comparatively small change in the higher π level from (2)—(4). This may be explained in terms of a simple model for OIT-n-B.[4,6,29] In that model, through-bond interactions involving π MOs arise through mixing of the symmetry-adapted combinations of π basis MOs with the highest occupied σ MO (HO-σ-MO), and the second highest occupied σ MO, (SHO-σ-MO). Because of symmetry constraints, one π combination will mix only with HO-σ-MO, whereas the other π combination will mix only with SHO-σ-MO. This (hyperconjugative) mixing results in both π levels being raised, the extent of which depends *directly* on the square of the coefficient of the hybrid sp^3 orbital AO_3 in the delocalized σ MO [see (27)], and *inversely* on the energy gap separating the σ and π MOs in question.[1b] Coefficients and energies of delocalized σ MOs may be obtained using the 'C' approximation.[30] It is then found that, as the number, n, of σ bonds is increased, the energies of both HO-σ-MO and SHO-σ-MO are raised, but that of the latter is affected more strongly, with the result that the two levels eventually converge. The coefficient of AO_3 in the HO-σ-MO, C_{HO}, is generally larger than that, C_{SHO}, in the SHO-σ-MO. However, C_{HO} and C_{SHO} respectively decrease and increase with increasing values of n.[4] Therefore, the energy level of that π combination which mixes with HO-σ-

MO will be relatively insensitive to the value of n (*both* C_{HO} and the energy gap *decrease* as n increases), whereas that of the other π combination, which mixes with SHO-σ-MO, is expected to increase with increasing n (C_{SHO} *increases*, energy gap *decreases*).

Laticyclic Hyperconjugation in (11a)—(13a).—The all-*trans* rule predicts that π-OIT-6-B, as measured by $\pi\Delta I_p$, should diminish along the series of dienes: (4) > (10) > (11a). Surprisingly, precisely the opposite sequence is observed, the $\pi\Delta I_p$ value for (11a) being 1.6 times larger than that found for (4), and even surpassing the $\pi\Delta I_p$ value for the five-bond diene (3). It is therefore extremely unlikely that OIT-6-B could account for such a large measured π-splitting energy for (11a). This belief is reinforced by the finding that $\pi\Delta I_p$ for the *cis-trans-trans-trans-trans-cis* eight-bond diene (12a) is 0.29 eV,' which is only marginally smaller than that found for the all-*trans* six-bond compound (4). From equation (1), the predicted $\pi\Delta I_p$ value for the all-*trans* eight-bond diene homologue of (4), arising from OIT-8-B, is only *ca.* 0.1 eV. Clearly, OIT-8-B should be even smaller for the diene (12a), and would, therefore, not be discernible by p.e. spectroscopy.

The origin of the large observed π-splitting energies for (11a) and (12a) is attributed to the presence of hyperconjugative interactions between the π MOs in these molecules and the $_w\pi$ MOs of the intervening CH_2 groups, as shown by (17). This type of hyperconjugation has been called laticyclic hyperconjugation[13] because of the laticyclic topology[31] displayed by the interacting MOs.

A simple model of laticyclic hyperconjugation has been developed,[13,19] the main features of which are shown in Figure 8. Laticyclic hyperconjugation in the dienes (11a)—(13a) is modelled by the ethene $\cdots (CH_4)_n \cdots$ ethene complexes ($n = $ 1—3), the geometries of which are identical to those of the corresponding fragments obtained from the crystal structures of (11b)—(13b). The HF/STO-3G computed energies and MO coefficients for the π and $_w\pi$ basis MOs are shown in the centre of Figure 8, and those for the MOs of the monomethane and dimethane complexes are respectively displayed on the right- and left-hand sides of that Figure. For the case of the monomethane complex, the level of the $\pi - \pi$ symmetry-adapted combination of π MOs is raised by 0.4 eV through mixing, in an antibonding fashion, with the $_w\pi$ MO of CH_4 as shown. The coefficients (H $1s$ and the C $2p$ orbitals) of the $_w\pi$ component in the resulting MO also reflect the large degree of
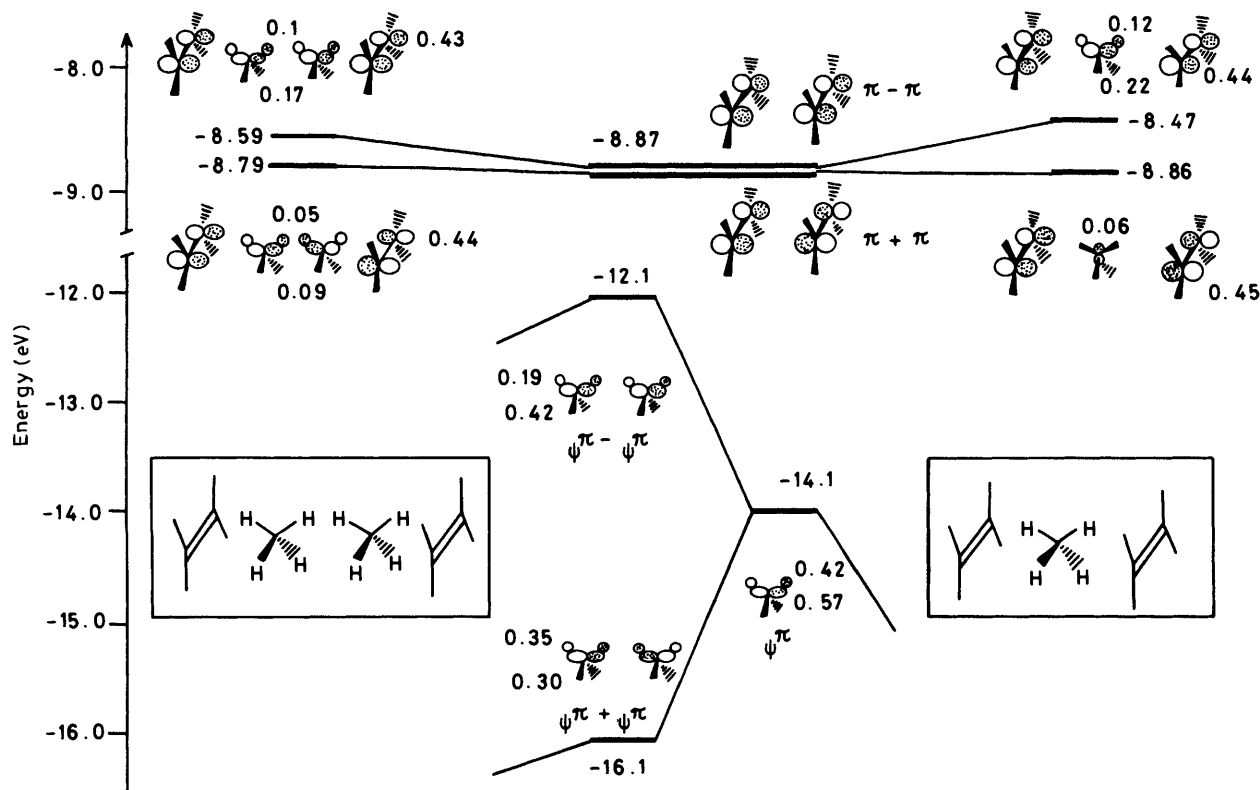
Figure 8. Energy correlation diagram for model complexes, the geometries of which were culled from the crystal structures of (**11b**) and (**12b**). Energies and MO coefficients are from HF/STO-3G calculations

mixing that obtains between the $\pi - \pi$ and $_\psi\pi$ basis orbitals. The corresponding $\pi + \pi$ combination cannot mix with the $_\psi\pi$ MO by dint of symmetry. It can, however, mix with a lower lying CH_4MO of a_1 symmetry (assuming C_{2v} point group symmetry), but because of overlap and energy gap considerations, this mixing is expected to be energetically negligible.[19] Indeed, the $\pi + \pi$ level is calculated to be raised by only 0.01 eV, and the resulting MO contains only a small contribution from the CH_4 a_1 orbital. The degeneracy of the π levels in the complex is therefore lifted, the calculated splitting energy being 0.39 eV.

For the case of the dimethane complex, two symmetry-adapted pairs of $_\psi\pi$ MOs can be formed, each of which is able to mix with one of the π combinations of the correct symmetry. Therefore, both $\pi + \pi$ and $\pi - \pi$ levels will now be raised. However, the $\pi - \pi$ level is more affected, largely because the energy gap between the $\pi - \pi$ and $_\psi\pi - _\psi\pi$ basis MOs is only about one half that separating the corresponding $\pi + \pi$ and $_\psi\pi + _\psi\pi$ MOs. The resulting $\pi - \pi$ level is lower in this complex than in ethene • • • CH_4 • • • ethene, presumably because the ratios of the squares of the coefficients in the single $_\psi\pi$ basis MO to those in the $_\psi\pi - _\psi\pi$ basis MO (1.8 : 1 for C and 4.9 : 1 for H) are larger than the ratio of the energy gap between $\pi - \pi$ and $_\psi\pi$ to that between $\pi - \pi$ and $_\psi\pi - _4\pi$ (1.6 : 1). Since both π levels in ethene • • • $(CH_4)_2$ • • • ethene are raised, the π-splitting energy for this complex is therefore smaller than that for ethene • • • CH_4 • • • ethene, and is calculated to be 0.20 eV.

Calculations on the trimethane complex, which models (**13a**), reveal that the $\pi - \pi$ and $\pi + \pi$ levels are respectively stabilized and destabilized with respect to the corresponding levels in the dimethane complex.[13] The resulting π-splitting energy is now only 0.11 eV, which would be too small to be discernible in the p.e. spectrum of (**13a**).

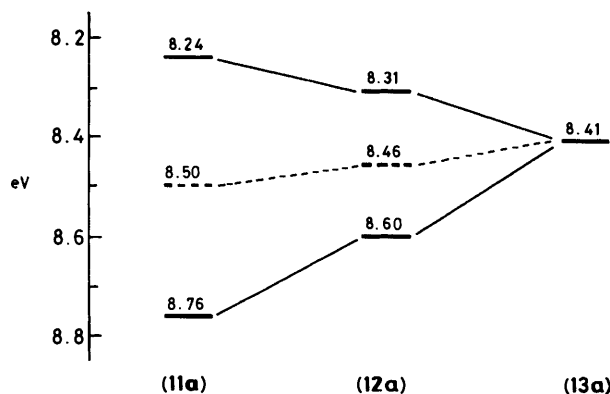It can be shown[13] that the π levels after laticyclic hyper-

Figure 9. πI_p Correlation diagram for (**11a**), (**12a**), and (**13a**). The dashed line connects the means of the πI_p values

conjugation follow the natural sequence,[32] that is, the $\pi - \pi$ combination lies above the $\pi + \pi$ combination, as shown in Figure 8. Since the natural sequence of levels also results from through-bond interactions occurring over an even number of relaying σ bonds (parity rule[2,4]), it follows that laticyclic hyperconjugation and OIT-n-B should reinforce each other in (**11a**)—(**13a**).

The trends in the π levels of these complexes are reproduced experimentally by the πI_p values for the dienes (**11a**)—(**13a**), which are shown by the correlation diagram of Figure 9. This correspondence suggests the involvement of laticyclic hyperconjugative interactions (and, presumably OIT-n-B) in these dienes.

The following experimental and calculational evidence unequivocally implicate the involvement of laticyclic interactions
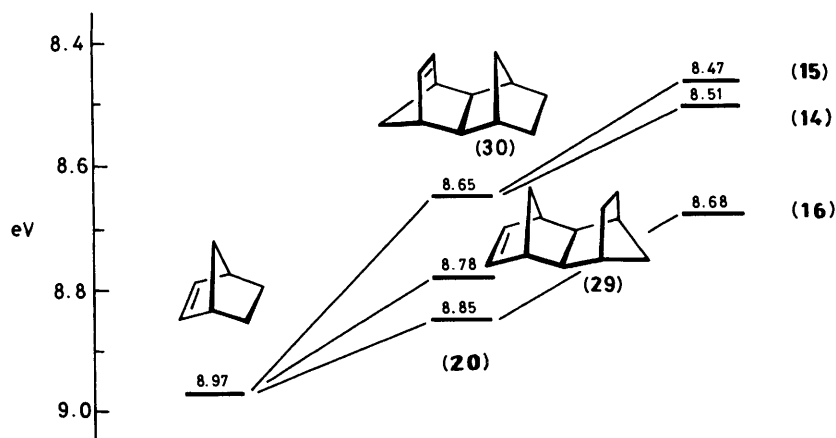
Figure 10. πI_p Correlation diagram for the monoenes norbornene, (14), (15), (16), (20), (29), and (30)

in (11a) and (12a). Inspection of the HF/STO-3G-computed $\pi - \pi$ MO of (11a) revealed it to contain a large (antibonding) contribution from the $_w\pi$ MO of the intervening CH_2 group. In fact, the coefficients of the fragment MOs in (11a) are practically identical to those in the model monomethane complex shown in Figure 8. No contribution from any MO associated with the central CH_2 group was evident in the corresponding $\pi + \pi$ MO. Both π MOs were found to contain a small contribution from the intervening σ bonds. Thus, it appears that both laticyclic hyperconjugation (major) and OIT-6-B (minor) are present in (11a).

The computed (STO-3G) π-splitting energy, ΔE_π, for (11a) is 0.51 eV (Table 11) which is, presumably, the sum of reinforcing laticyclic hyperconjugative and OIT-6-B contributions. The laticyclic contribution may be approximated by that calculated for the monomethane complex of Figure 8, i.e. 0.39 eV. The OIT-6-B contribution may be equated with the (STO-3G) calculated π-splitting energy of 0.18 eV for (28), in which laticyclic hyperconjugation is necessarily absent. The sum of the individual (reinforcing) laticyclic and OIT-6-B interactions amounts to 0.57 eV, which agrees well with the overall calculated ΔE_π value of 0.51 eV for (11a).

The experimental data also support this analysis. The $\pi\Delta I_p$ value for (28) is ca. 0.17 eV (Table 11), which may be equated with the OIT-6-B contribution in (11a). Subtraction of this quantity from the $\pi\Delta I_p$ value of 0.52 eV for (11a) yields a laticyclic hyperconjugative contribution of 0.35 eV, which agrees with the calculated value above.

The agreement between these results and those obtained theoretically leads us to conclude confidently that laticyclic hyperconjugation and OIT-6-B in (11a) amount to ca. 0.35 and 0.17 eV respectively. Laticyclic hyperconjugation is therefore responsible for about 70% of the total π-splitting energy observed for (11a). Another important result from the above analysis is that through-six-bond interactions in (11a) are, in fact, considerably smaller than those in (4), thereby providing further confirmation of the all-*trans* rule.

The examination of the π^* levels in (11a)[29] should provide a particularly stringent test of the laticyclic hyperconjugation theory. For reasons of symmetry, laticyclic interactions should be *absent* in the π^* orbitals of (11a) (because the $_w\pi$ orbital is symmetric with respect to the plane of symmetry containing the major molecular axis, whereas the π^* MOs are antisymmetric with respect to this plane). Calculations on the monomethane complex also predict negligible splitting of the π^* levels. Indeed, the e.t. spectrum of (11a) showed no evidence of any enhanced π^*-splitting, relative to that observed for (28),[29] thereby

providing further support that laticyclic hyperconjugation is largely responsible for the large observed $\pi\Delta I_p$ value for (11a).

From the $\pi\Delta I_p$ value for (12a) and the calculated π-splitting energy for the dimethane complex (Figure 8), laticyclic hyperconjugation and OIT-8-B contribute ca. 0.20 and 0.09 eV respectively to the observed π-splitting energy in (12a). Orbital interactions in (12a) could not be explored directly using the HF/STO-3G model because of basis set size limitations. However, PRDDO MO calculations were carried out on this molecule, but the computed ΔE_π value was found to be 0.15 eV, only one half of that found experimentally. It is our experience[12] that the PRDDO method underestimates through-bond, and presumably also laticyclic, interactions by as much as a factor of two. Notwithstanding this discrepancy, the PRDDO $\pi + \pi$ and $\pi - \pi$ MOs (of (12a) are practically identical to the respective MOs of the dimethane complex of Figure 8, thereby strengthening our conviction that significant laticyclic interactions are present in (12a). Such laticyclic effects in this molecule are surprisingly large, considering that they are transmitted over a distance of ca. 9 Å by a relay of two methano groups held 3 Å apart!

The combined effects of laticyclic hyperconjugation and OIT-10-B in (13a) are estimated to be no more than 0.15 eV. Unfortunately, the p.e. spectrum of (13a) showed only a single broad πI_p band appearing as a hump on the σ onset [Figure 6(ii)], thereby effectively masking any small splitting (of the order of 0.1 eV) that could be present.

Laticyclic hyperconjugation can, of course, occur also in the corresponding monoenes,[13] and this is revealed by the πI_p correlation diagram for several of such compounds, shown in Figure 10. The πI_p value was found to decrease along the series: 8,9,10-trinorbornene > (20) > (16). This trend probably reflects increasing hyperconjugative interactions of the kind shown by (27). Thus, an increase in the length of the σ bond framework is accompanied by a corresponding elevation of the highest lying σ MO levels, and a consequent narrowing of the σ–π energy gap. Presumably, such an effect is also present in the monoenes (30), (14), and (15), which accounts for the difference between the πI_p values for (30) and (15) being almost identical to that between (20) and (16). However, the πI_p values for (30) and (15) [and (14)] are raised by the same amount, ca. 0.2 eV, relative to (20) and (16) respectively. This extra lowering, by 0.2 eV, of the πI_p for (30), (14), and (15) is attributed to laticyclic hyperconjugative interactions in these molecules, involving improved orbital overlap between the double bond and the closest CH_2 group which must necessarily be much smaller in norbornene, (20) and (16). It can easily be shown that laticyclic

hyperconjugative interactions involving a CH_2 group and two double bonds, having the configuration shown by (11a), should be double those involving just one double bond, as in (30), (14), or (15).[13] Using the value of 0.2 eV, determined for monoenes such as (30), laticyclic hyperconjugation in (11a) is estimated to be 0.4 eV, which is in excellent agreement with the value of 0.35 eV obtained by other means (vide supra). Furthermore, the mean of the two πI_p values for (11a) (see Figure 9), 8.50 eV, is identical to the πI_p value of 8.51 eV observed for (14), a result which again is totally consistent with the operation of laticyclic hyperconjugation in both the diene and the monoene.

A quantitative analysis of orbital interactions in the diene (10) is difficult because the double bonds are located in different environments. Thus, laticyclic interactions in this molecule are not simply twice those in (15) because each of the $\pi + \pi$ and $\pi - \pi$ combinations (10) is now able to mix with both $_w\pi - _w\pi$ and $_w\pi + _w\pi$ MOs of the two CH_2 fragments. This is a consequence of the large difference in the orbital overlap between the two double bonds with their nearest neighbour CH_2 groups. The degree of mixing is therefore only slightly affected by the nodal properties of the π combinations. Since both $\pi + \pi$ and $\pi - \pi$ levels are expected to be shifted by comparable amounts, it follows that the π-splitting energy in (10), caused by laticyclic interactions, should be quite small, but just how small it is cannot be estimated from the present data alone. HF/STO-3G calculations on a model ethene $\cdots$ $(CH_2)_2 \cdots$ ethene complex whose geometry mimics the salient features of (10) are of no help here because of the unrealistic proximity between the two pairs of hydrogen atoms (<0.8 Å apart) attached to the ethene and CH_4 molecules that model the left-hand-side half of (10). The problem can be tackled experimentally through measurement of the $\pi\Delta I_p$ value for the diene having the overall structure of (10), but lacking the central CH_2 bridge. This would provide an estimate of OIT-8-B in (10). Subtraction of this quantity from $\pi\Delta I_p$ for (10) would give an estimate of laticyclic interactions within this molecule.

Long-range Nature of Laticyclic Hyperconjugative Interactions.—Although the paucity of experimental data prevents a quantitative distance dependence of laticyclic hyperconjugation to be made, it is evident from the p.e. data for (12a) that such interactions can extend over large distances. HF/STO-3G calculations[13] on an extended series of complexes of the type shown in Figure 8 indicate an approximate exponential decay of laticyclic interactions with respect to the number, n, of intervening methane groups (spaced 3 Å apart) according to the equation:

$$\ln \Delta E_\pi = -0.69n - 0.248 \qquad (2)$$

from which a splitting energy of ca. 10^{-3} eV is predicted for $n = 10$, or equivalently, for an ethene–ethene separation of ca. 33 Å! Therefore, laticyclic hyperconjugation, like OIT-n-B [equation (1)], appears to be a very long-range process indeed.

Although a splitting energy of 10^{-3} eV is negligible from a p.e. spectroscopic point of view, it can have a dramatic effect on the rates of electron-transfer processes. Assuming that ΔE_π is approximately equal to twice the value of the electron coupling (transfer) integral J,[33] then a splitting energy of 10^{-3} eV between cation radical states could give rise to rates of up to 10^9 sec^{-1} for intramolecular electron-transfer within the ground-state cation radical.[33] Thus, it appears that through-bond and laticyclic interactions, operating respectively through a relay of σ bonds, and through a series of discrete alkane groups that are in van der Waals contact (ca. 3.2 Å), could provide mechanisms for promoting extremely rapid rates of intramolecular electron-transfer between donor and acceptor moieties separated by distances as large as 20—30 Å. Indeed, we believe that through-

bond effects must be responsible for the observed rapid rates of photoinduced intramolecular electron-transfer (10^8—10^{11} sec^{-1}) in systems in which the chromophores are separated by distances of up to 14 Å.[7,8,34—36]

It is therefore of considerable interest that the recently resolved structure of the photosynthetic reaction centre of *Rhodopseudomonas viridis*[37] shows that the phytyl side chains of both the special chlorophyll pair and menaquinone to be in van der Waals contact with a bacteriopheophytin molecule. This situation is somewhat akin to a long-chain alkane group placed in between a donor and acceptor pair. Recent HF/STO-3G calculations[38] on a series of complexes of the type ethene $\cdots C_nH_{2n+2} \cdots$ ethene ($n = 1$—11), in which an ethene group is placed 3.6 Å from each end of an n-alkane molecule in its fully staggered, antiperiplanar conformation, reveal only a mild attenuation of ΔE_π with the length of the alkane, e.g. $\Delta E_\pi = 0.02$ eV when the alkane is $C_{11}H_{24}$, corresponding to an ethene–ethene separation in the complex of ca. 20 Å! Such a splitting energy could therefore give rise to rates of intramolecular electron-transfer within the ground-state cation radical of the C_{11}-alkane complex of up to 10^{11} s^{-1}.[33] These predicted rates are comparable to those that are actually found to occur in the photosynthetic reaction centre.[7a] Notwithstanding the crudeness of the model complex, the results do suggest the intriguing possibility that the phytyl side chains in the photosynthetic reaction centre might, through laticyclic or through-bond interactions, play a crucial role in promoting electron transport, that is, by acting as an electron 'conductor'. Perhaps the protein molecules that surround the redox sites in the reaction centre also provide a through-bond pathway for electron transport. Such speculations are obviously worthy of further investigation.

Conclusion

The following important points emerge from this study. (i) The p.e. data for the series of dienes (1)—(4) provide convincing evidence for the long-range nature of OIT-n-B. Such interactions can be as large as 10^{-3} eV even for $n = 18$ bonds.

(ii) The observed π-splitting energy of 0.52 eV for (11a) is considerably larger than that (0.32 eV) found for (4). This apparent violation of the all-*trans* rule is a result of the presence of large laticyclic hyperconjugative interactions (0.35 eV) in (11a). Through-six-bond interactions in (11a) are therefore only 0.17 eV, and are indeed smaller than those found in (4).

(iii) Laticyclic hyperconjugation was also found to be important in (12a), amounting to ca. 0.20 eV. This is a surprisingly large result considering the large distance (9 Å) separating the double bonds in this compound. The predicted π-splitting energy for (13a), resulting from combined laticyclic and through-bond interactions, is too small to be detectable by p.e. spectroscopy.

(iv) Crystal structures of (11b)—(13b) revealed the proximity (ca. 3 Å) between the nearest neighbours within the set of double bonds and the intervening CH_2 groups. Such structurally enforced propinquity produces optimal laticyclic hyperconjugation in these dienes.

(v) HF/STO-3G calculations on model complexes reveal the long-range nature of laticyclic hyperconjugation. Perhaps such interactions, together with OIT-n-B, play a vital role in facilitating electron-transfer processes in biological systems. This possibility is being pursued further by one of us (M. N. P.-R.) and the results of these studies will appear in due course.

References

1 (a) F. Brogli, W. Eberbach, E. Haselbach, E. Heilbronner, V. Hornung, and D. M. Lemal, *Helv. Chim. Acta*, 1973, **56**, 1933; (b) M. N. Paddon-Row, H. K. Patney, R. S. Brown, and K. N. Houk, *J. Am. Chem. Soc.*, 1981, **103**, 5575; (c) M. N. Paddon-Row, H. K. Patney, J. B. Peel, and G. D. Willett, *J. Chem. Soc., Chem. Commun.*, 1984, 564; (d) F. S. Jørgensen, M. N. Paddon-Row, and H. K. Patney, *ibid.*, 1983, 573.

2 R. Hoffmann, *Acc. Chem. Res.*, 1971, **4**, 1.

3 R. Gleiter, *Angew. Chem., Int. Ed. Engl.*, 1974, **13**, 696.

4 M. N. Paddon-Row, *Acc. Chem. Res.*, 1982, **15**, 245.

5 T. Koopmans, *Physica*, 1934, **1**, 104.

6 M. N. Paddon-Row, E. Cotsaris, and H. K. Patney, *Tetrahedron*, 1986, **42**, 1779.

7 *Inter alia*: (a) J. Jortner, *J. Am. Chem. Soc.*, 1980, **102**, 6676; (b) L. T. Calcaterra, G. L. Closs, and J. R. Miller, *ibid.*, 1983, **105**, 671.

8 N. S. Hush, M. N. Paddon-Row, E. Cotsaris, H. Oevering, and J. W. Verhoeven, *Chem. Phys. Lett.*, 1985, **117**, 8.

9 J. M. Warman, M. P. de Haas, M. N. Paddon-Row, E. Cotsaris, N. S. Hush, H. Oevering, and J. W. Verhoeven, *Nature*, 1986, **320**, 615.

10 R. Hoffmann, A. Imamura, and W. J. Hehre, *J. Am. Chem. Soc.*, 1968, **90**, 1499.

11 H.-D. Martin and R. Schwesinger, *Chem. Ber.*, 1974, **107**, 3143.

12 F. S. Jørgensen and M. N. Paddon-Row, *Tetrahedron Lett.*, 1983, **24**, 5415.

13 M. N. Paddon-Row, *J. Chem. Soc., Perkin Trans. 2*, 1985, 257.

14 D. D. Chau, M. N. Paddon-Row, and H. K. Patney, *Aust. J. Chem.*, 1983, **36**, 2423.

15 J. A. Ibers and W. C. Hamilton (eds.), 'International Tables for X-Ray Crystallography,' vol. IV, The Kynoch Press, Birmingham, 1984.

16 J. M. Stewart and S. R. Hall (eds.), 'The XTAL system of Crystallographic Programs: User's Manual,' Technical report TR-901, Computer Science Center, University of Maryland, U.S.A., 1983.

17 C. K. Johnson, 'ORTEP-II,' Oak Ridge National Laboratory, Tennessee, U.S.A., 1976.

18 T. P. DeLacy and C. H. L. Kennard, *J. Chem. Soc., Perkin Trans. 2*, 1972, 2153.

19 D. C. Craig, M. N. Paddon-Row, and H. K. Patney, *Aust. J. Chem.*, 1986, **39**, 1587.

20 N. G. Rondan, M. N. Paddon-Row, P. Caramella, and K. N. Houk, *J. Am. Chem. Soc.*, 1981, **103**, 2436.

21 G. Wipff and K. Morokuma, *Tetrahedron Lett.*, 1980, **21**, 4445.

22 A. A. Pinkerton, D. Schwarzenbach, J. H. A. Stibbard, P.-A. Carrupt, and P. Vogel, *J. Am. Chem. Soc.*, 1981, **103**, 2095.

23 W. H. Watson, J. Galloy, P. D. Bartlett, and A. A. M. Roof, *J. Am. Chem. Soc.*, 1981, **103**, 2022.

24 P. D. Bartlett, A. J. Blakeney, M. Kimura, and W. H. Watson, *J. Am. Chem. Soc.*, 1980, **102**, 1383.

25 O. Ermer and S. A. Mason, *J. Chem. Soc., Chem. Commun.*, 1983, 53.

26 E. L. Eliel, N. L. Allinger, S. J. Angyal, and G. A. Morrison, 'Conformational Analysis,' Wiley-Interscience, New York, 1965, ch. 7.

27 T. A. Halgren, D. A. Kleier, J. H. Hall, Jr., L. D. Brown, and W. N. Lipscomb, *J. Am. Chem. Soc.*, 1978, **100**, 6595.

28 N. L. Allinger and Y. H. Yuh, *Q.C.P.E.*, 1980, **13**, 395.

29 V. Balaji, L. Ng, K. D. Jordan, M. N. Paddon-Row, and H. K. Patney, *J. Am. Chem. Soc.*, in press.

30 C. Sandorfy and R. Daudel, *C.R. Hebd. Seanses Acad. Sci.*, 1954, **238**, 93.

31 M. J. Goldstein and R. Hoffmann, *J. Am. Chem. Soc.*, 1971, **93**, 6193.

32 E. Heilbronner and A. Schmelzer, *Helv. Chim. Acta*, 1975, **58**, 936.

33 N. S. Hush, *Coord. Chem. Rev.*, 1985, **64**, 135.

34 J. M. Warman, M. P. de Haas, H. Oevering, J. W. Verhoeven, M. N. Paddon-Row, A. M. Oliver, and N. S. Hush, *Chem. Phys. Lett.*, 1986, **128**, 95.

35 J. W. Verhoeven, M. N. Paddon-Row, N. S. Hush, H. Oevering, and M. Heppener, *Pure Appl. Chem.*, 1986, **58**, 1285.

36 H. Oevering, M. N. Paddon-Row, M. Heppener, A. M. Oliver, E. Cotsaris, J. W. Verhoeven, and N. S. Hush, *J. Am. Chem. Soc.*, 1987, **109**, 3258.

37 J. Deisenhofer, O. Epp, K. Miki, R. Huber, and H. Michel, *J. Mol. Biol.*, 1984, **180**, 385.

38 M. N. Paddon-Row, unpublished data.